Ice Surface Temperature Retrieval from AVHRR, ATSR, and Passive Microwave Satellite Data: Algorithm Development and Application

NAGW-3437

YEAR 2 ANNUAL REPORT

Jeff Key
James Maslanik
Konrad Steffen

Cooperative Institute for Research in Environmental Sciences
University of Colorado at Boulder

March 24, 1995

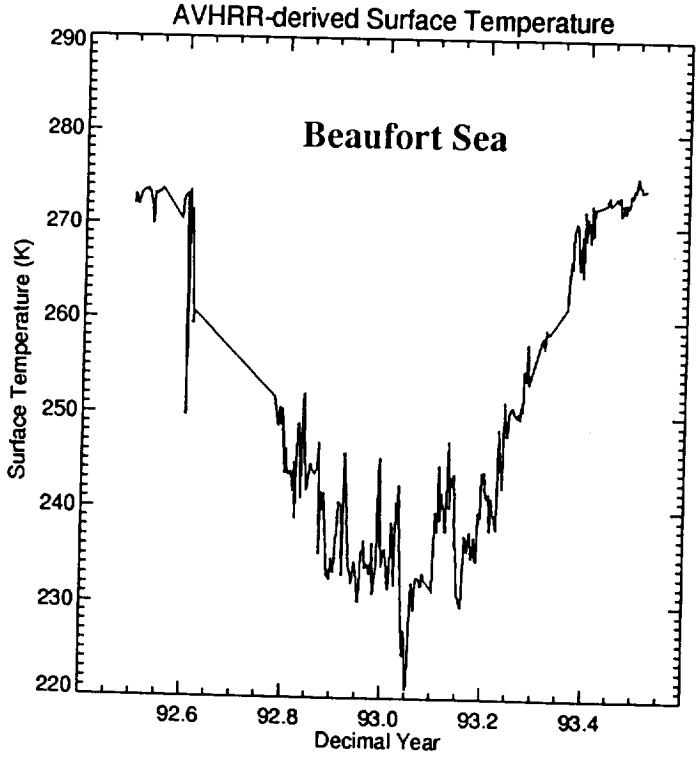

TABLE OF CONTENTS

SUMMARY

During the second project year we have made progress in the development and refinement of surface temperature retrieval algorithms and in product generation. More specifically, we have accomplished the following:

- acquired a new AVHRR data set for the Beaufort Sea area spanning an entire year,
- acquired additional ATSR data for the Arctic and Antarctic now totalling over eight months,
- refined our AVHRR Arctic and Antarctic ice surface temperature (IST) retrieval algorithm, including work specific to Greenland,
- developed ATSR retrieval algorithms for the Arctic and Antarctic, including work specific to Greenland,
- developed cloud masking procedures for both AVHRR and ATSR,
- generated a two-week bi-polar GAC set of composite images from which IST is being estimated,
- investigated the effects of clouds and the atmosphere on passive microwave "surface" temperature retrieval algorithms, and
- generated surface temperatures for the Beaufort Sea data set, both from AVHRR and SSM/I.

During Year 3 we will focus on product generation, making refinements to cloud masking, temperature retrieval, and data processing methods as necessary.

INTRODUCTION

One essential parameter used in the estimation of radiative and turbulent heat fluxes from satellite data is surface temperature. Sea and land surface temperature (SST and LST) retrieval algorithms that utilize the thermal infrared portion of the spectrum have been developed, with the degree of success dependent primarily upon the variability of the surface and atmospheric characteristics. However, little effort has been directed to the retrieval of the sea ice surface temperature (IST) in the Arctic and Antarctic pack ice or the ice sheet surface temperature over Antarctica and Greenland. The goal of this research is to increase our knowledge of surface temperature patterns and magnitudes in both polar regions, by examining existing data and improving our ability to use satellite data as a monitoring tool. Four instruments are of interest in this study: the AVHRR, ATSR, SMMR, and SSM/I. Our objectives are to

1. Refine the existing AVHRR retrieval algorithm defined in *Key and Haefliger* (1992; hereafter KH92) and applied elsewhere.
2. Develop a method for IST retrieval from ATSR data similar to the one used for SST.
3. Further investigate the possibility of estimating surface temperature from passive microwave data (in conjunction with AVHRR clear sky samples) through the use of "effective emissivities" and physical relationships between skin temperature and subsurface temperature.
4. Calculate a 12-year record of clear sky equivalent surface temperatures, or possibly all-sky snow-ice interface physical temperatures, from SMMR and SSM/I, compare these temperatures to climatologies, ECMWF modeled surface temperatures, and surface temperatures predicted by a 2-D ice model.
5. Intercompare several ice surface retrieval methods and validate them against ground measurements from the Swiss Camp on the Greenland ice sheet.

Additionally, we intend to develop a surface temperature product based on AVHRR data and possibly blended with drifting buoy and meteorological station temperatures. However, the temporal coverage of this product will depend upon the availability of data from the Pathfinder activity. Discussions are underway with scientists from a number of agencies/institutes to coordinate our activities.

This document summarizes our progress during the second project year.

1.0 PROGRESS TO DATE: DATA ACQUISITION

1.1 AVHRR Coverage

We are basing all of our AVHRR surface temperature work on the following data sets:

- daily imagery for the Beaufort Sea for June 1992 to July 1993, acquired and processed as part of a separate NASA grant for ice motion studies from AVHRR,
- data acquired during LEADEX and the SIMMS field experiments,

- two weeks of GAC data during summer and winter of 1984.

We were investigating the possibility of acquiring a multi-year polar GAC subset from the Pathfinder data set at JPL. Due to the computationally intensive nature of this task, we had hoped to work with NSIDC for low-level processing. Unfortunately, acquiring large quantities of data will probably not be possible this way. A proposal has been submitted under the AVHRR Pathfinder announcement of opportunity to acquire and process the 12-year record of GAC data. Additionally, we hope to acquire a one-year GAC data set being compiled for an ice motion study under separate NASA funding.

1.2 ATSR

ATSR data are being acquired for algorithm validation purposes only. Data continue to be sent to J. Key from from Rutherford Appleton Laboratory (England) for times and locations corresponding to recent field experiments. Coverage of one month in four Arctic and one Antarctic locations was originally requested; we now have over eight months of data for each region (well over 100 tapes). Six of the months overlap with the Beaufort Sea AVHRR data set.

2.0 PROGRESS TO DATE: METHODS

2.1 Estimates of IST Using Thermal Data: Basin-wide Algorithms

AVHRR and ATSR radiance simulations using the LOWTRAN-7 radiative transfer model have been completed using the recently-acquired Arctic and Antarctic radiosonde data and emissivity measurements (Figure 1). The form of the surface temperature predictive equation has changed slightly in order to be more consistent with that used in sea surface temperature retrievals. We have switched from seasonally-dependent formulae to temperature-dependent. Sensitivity studies concerning the effects of spring aerosol loading, surface melt, and geographic variations in total precipitable water are in progress.

Figure 2 shows the clear sky surface temperature for the Beaufort Sea 1992-93 data set, ECMWF 1013 mb (near surface) temperatures, and temperature from the recently-developed "POLES" data set (Munoz and Martin, 1995). The ECMWF temperatures are model forecasts, and incorporate Soviet drifting ice station soundings when and where available. The POLES temperature data utilize buoy temperatures, land station temperatures, and drifting ice station temperatures. Both the ECMWF and POLES data are for all-sky conditions, in contrast to the AVHRR-derived data which are only for clear sky areas. While all three time series exhibit similar patterns, the differences in magnitude are dramatic. The AVHRR-derived temperatures are by far the lowest. This is to be expected because temperatures near the surface are generally higher under cloud cover, except in mid-summer. Also, surface temperatures will usually be lower than 2 m air temperatures over the ice pack as a result of frequent low-level inversions, though this difference is generally less than one degree. The accuracy of the buoy temperatures is also in question since they are subject to heating by solar radiation during the summer, and may be snow-covered and therefore insulated during the winter. While there is certainly some inherent error in the

AVHRR retrievals, this is most likely on the order of 1-2K rather than the 5-15K differences shown in the figure.

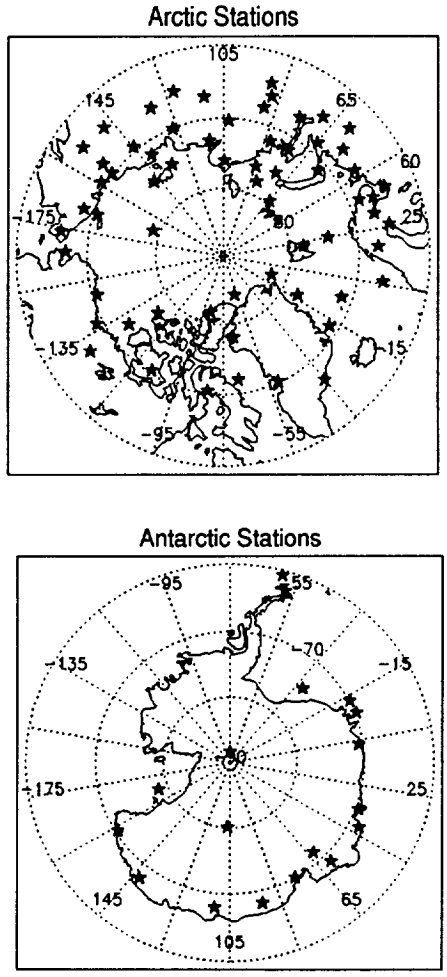

Fig. 1. Arctic and Antarctic stations for which radiosonde data are available.

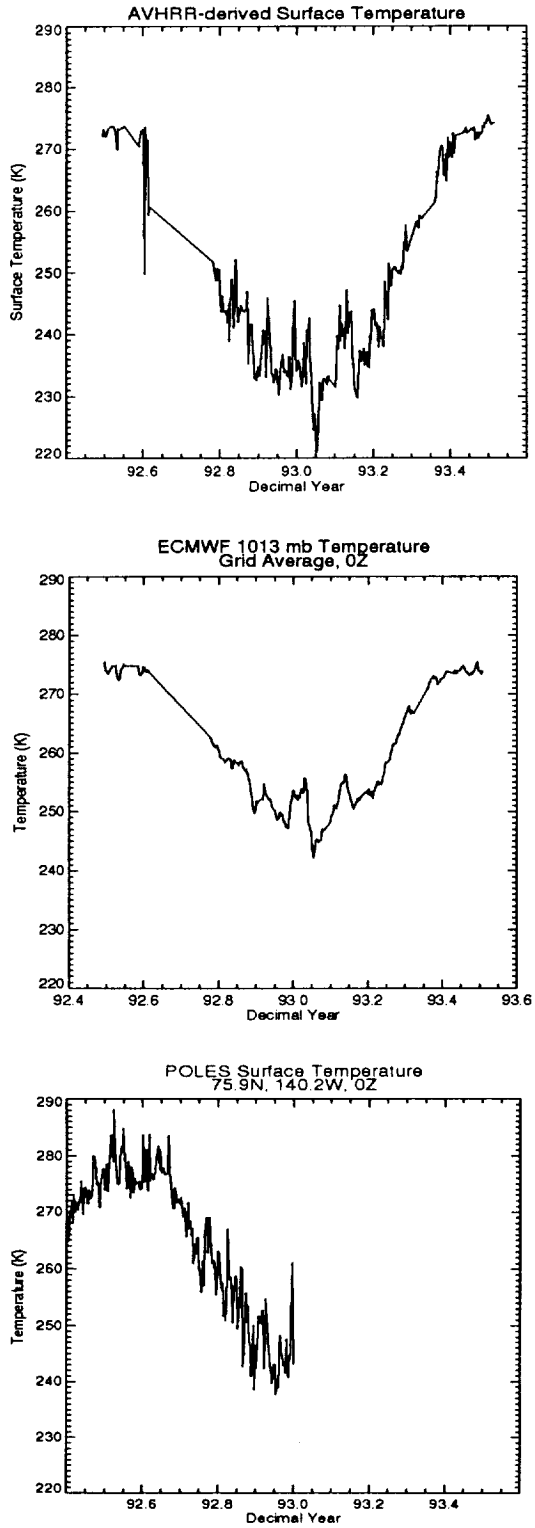

Fig. 2. Clear sky surface temperatures over the Beaufort Sea computed from daily AVHRR LAC data (top), 1013 mb temperatures from ECMWF (middle), and surface temperatures from the POLES temperature data set (bottom). There is a two month gap from mid-August to mid-October 1992 in the AVHRR and ECMWF data sets.

Cloud detection in satellite data is the largest obstacle in the path of accurate surface temperature estimation, and is most difficult in the polar regions where surface temperatures and reflectances are often very similar to those of the cloud tops. Two cloud detection methods, the difference between them being the type of input data, have recently been developed and incorporated into the Cloud and Surface Parameter Retrieval (CASPR) system (developed under separate NASA funding). As part of this project, the AVHRR procedures have been modified for use with the ATSR.

2.2 Surface Temperature Retrieval Over Greenland With ATSR

In a manner similar to the retrieval of surface temperature for the polar regions described in Section 2.1, a method has been developed for estimating the surface temperature specifically for the Greenland ice sheet using the ATSR. The dual-angle capability of ATSR is expected to give a significant improvement in surface temperature accuracy.

Unlike the methods described in the previous section, the surface temperature used in the model simulations of ATSR radiances was calculated after the Stefan-Boltzmann law ($L = \sigma T^4$) using the measured outgoing longwave radiation measured at the camp. Since the uncertainty of the measurements is given as 3% this amount was added and subtracted, respectively, to each measured value. This way two additional profiles were created to every original clear sky profile, which differ only through different surface temperatures.

Figure 3 shows the estimated surface temperature calculated from the modeled 11 micron brightness temperatures compared to the observed surface temperature. The RMS error for this model is 0.26K. From the graph it is apparent that there are a few cases where the modeled surface temperatures are underestimated. This could be due to clouds that were not visible but were in the radiosonde profile. This could also be a result of only using summer profiles. During periods of very low water vapor concentrations the ratio of absorption in each channel does not remain in proportion because absorption by CO_2 begins to dominate. In such cases we would expect the split-window technique to break down. In addition, no variations in aerosol concentrations were included, which is also expected to cause the split-window technique to be less accurate. Efforts are currently underway to re-run the LOWTRAN model for different aerosol loadings and different seasons.

2.3 Passive Microwave-Derived Ice Temperatures

Cloud cover and atmospheric water vapor limit the usefulness of optical-wavelength data such as AVHRR for ice temperature retrievals. While also affected by clouds and water vapor, passive microwave data provide surface information under all polar atmospheric conditions, and thus are potentially valuable for ice temperature retrievals. The objective of this task is to define the utility of passive microwave data for sea ice temperature estimates. The main uncertainties controlling the usefulness of microwave data for IST retrievals are atmospheric effects and errors due to estimates of surface type mixtures and emissivities for each type.

Results of radiative transfer modeling for the examination of atmospheric effects were given in the previous report. From these results, we estimated that atmospheric water was likely to introduce errors in 19 Ghz vertical-polarization brightness temperatures of about 1.5 degrees. To test the reality of this, we have analyzed SSM/I data for the Seasonal Sea Ice Monitoring and Modeling Site (SIMMS) experiment for 1993, located near Resolute Bay in the Canadian Archipelago. The SIMMS data set includes thermistor-measured temperatures within the snow and ice column, as well as detailed cloud observations and meteorological measurements. SSM/I data were extracted from individual orbits and were supplied by NSIDC.

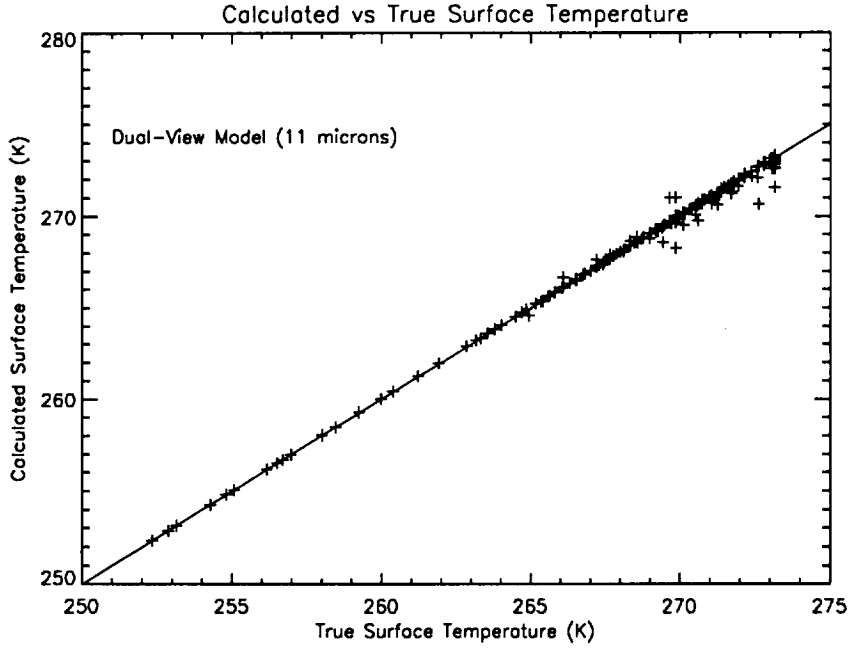

Fig. 3. Surface temperatures derived from surface based observations and from the ATSR thermal channels over the CIRES camp on the Greenland ice sheet.

Figure 4 compares the observed snow/ice interface temperature, SSM/I IST estimated using 19V (assuming 100% first-year ice concentration and an emissivity estimated from the mean 19V TB and observed temperature), and 19V IST estimated using emissivities assigned to ice concentration types calculated using the NASA Team Algorithm with global tie points. The correlation of TB with measured temperature is high; indicating that in spite of the large field of view of the SSM/I, the SSM/I data track the measured temperatures quite well. Correlations are significant for all levels in the snow column and the upper surface of the ice. The maximum correlation between measured temperatures and SSM/I TB occurs for temperatures at the snow/ice interface for both 19V and 37V. Corre-

lations are slightly higher for 19V than for 37V (Pearson's correlation coefficients of 0.96 at 19V and 0.94 at 37V at the snow/ice interface).

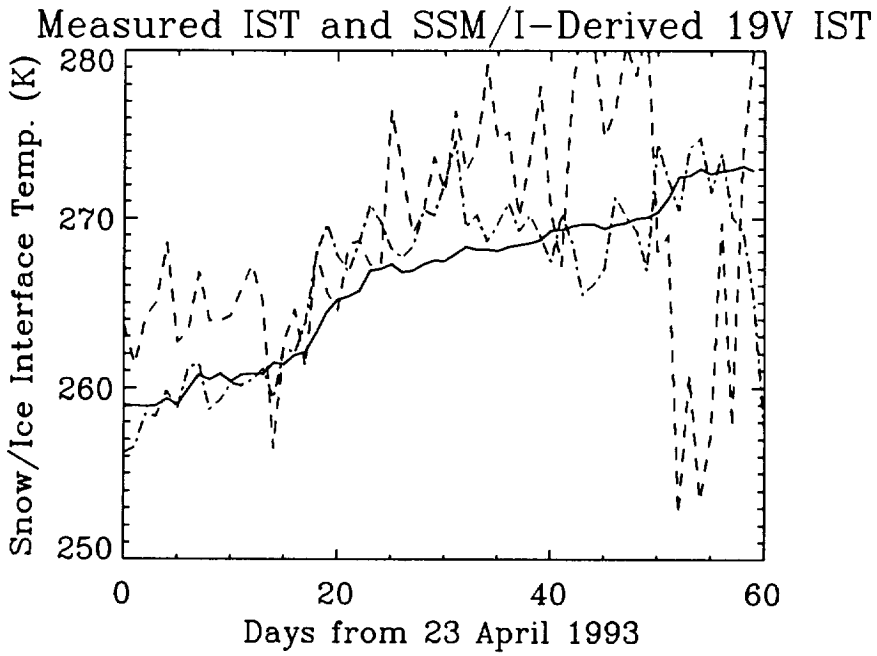

Fig. 4. Comparison of ice temperatures observed for the SIMMS field site. The solid line is the measured snow/ice interface temperature. The dot-dashed line is the temperature estimated from SSM/I 19 GHz V data, assuming 100% ice concentration and an emissivity estimated from the mean of the observed temperatures. The dashed line is SSM/I-derived temperature estimated using output from the NASA Team Algorithm for ice type proportions, and emissivities taken from the literature for open water, first-year ice, and multiyear ice.

The day-to-day variability in the SSM/I TBs is greater than that seen in the measured temperatures. This variability could be due to changing surface conditions, atmospheric effects, and to variations in the precise coverage of the SSM/I field of view from orbit to orbit to include differing proportions of snow-covered land and, perhaps, some open water at the ice edge in Lancaster Sound). Comparisons with cloud cover observations (cloud type, fraction, and opacity) show that increases in SSM/I TB occur during periods with thick stratus cloud. The snow/ice interface temperatures also increase during these events, as expected due to increased downwelling longwave radiation, but the change, even at the surface, is less than seen in the SSM/I TBs. The increases in 19V and 37V TB are comparable to those simulated using RADTRAN for stratus cloud. We therefore conclude that the variability of 1 to 3 K is due primarily to cloud cover. The large errors near the end of the time series in Figure 4 are due to a false, large multiyear ice signal. In spite of this variability, the SSM/I data clearly are capable of capturing the general temporal patterns of the temperatures. If the surface type and emissivity are known (a big "if"), then the

passive microwave data apparently can provide quite realistic snow/ice interface temperatures.

The positive bias in the Team Algorithm-derived temperatures can be reduced by assigning higher emissivities to one or more of the surface types or by applying some a priori knowledge about the ice conditions. For example, if we assume that the ice cover is known to be 100% but that the ice type mixtures are unknown (e.g., we use the Team Algorithm ice type estimate but set the total concentration to 100%, such as for the central Arctic in winter), then the 19V ISTs improve substantially (Figure 5). Setting the multi-year ice fraction to zero improves the estimates somewhat, but not as much as when the total ice concentration is corrected. If ice temperatures are known (such as from AVHRR), then the adjustment to bring the SSM/I-derived ISTs in line with the AVHRR ISTs actually provides a potential means to improve the SSM/I ice concentration estimates. Such adjustments essentially amount to a local tuning of the Team Algorithm.

These results for the SIMMS site suggest the following: 1) atmospheric effects are not prohibitive; 2) brightness temperatures are closely related to measured snow/ice and snow column temperatures; and 3) uncertainties in surface type and emissivity cause significant errors. To explore the SSM/I applications further, SSM/I ISTs were calculated for the Beaufort Sea AVHRR time series, with the SSM/I data resampled to the AVHRR grid size. The SSM/I-derived ISTs were then compared to AVHRR-derived IST and cloud cover. Temperatures were also available from two drifting buoys within the study region. In this case, we are comparing skin temperatures from AVHRR and some mix of skin temperature and snow temperature from the drifting buoy with the probable snow/ice interface temperature sensed by the SSM/I data.

Comparisons of the SSM/I-derived IST to the clear-sky AVHRR-derived IST for the Beaufort Sea time series suggest some similarities with the SIMMS experiment. In this case, the SSM/I ISTs were calculated by assigning emissivities to ice concentrations estimated using the NASA Team algorithm, with emissivities taken from the literature. As with the SIMMS case, the SSM/I data show greater variability, but some similarity to the AVHRR time series, although biased upward substantially.

As with the SIMMS case, the SSM/I-derived ISTs can be brought more closely in line with the AVHRR temperatures by adjusting the Team Algorithm results and/or assigning different emissivities to the surface types. For example, in Figure 6, the SSM/I temperatures were adjusted by prescribing that some of the estimated open-water fraction was in fact thin/young ice (a realistic assumption) and that ice emissivities where about 10% higher than quoted in the literature. A fixed change in young-ice fraction and emissivity were applied to the entire time series. The observations could obviously be made to agree exactly if adjustments were made for each point. The change in temperatures at about day 22 (12 March) may indicate the expected reversal in the snow temperature profile (as also shown in the SIMMS data above), when the energy input at the surface becomes greater than that from beneath the ice.

In addition to these comparisons using the NASA Team algorithm method, two additional SSM/I IST algorithms were explored. The first of these involved using AVHRR IST to

estimate emissivities that were then supplied to the Team Algorithm surface-type mixtures. An attempt was also made to derive emissivities using multiple linear equations as described in the previous report. However, the set of equations was not constrained enough to be solvable for mixtures of three possible surface types.

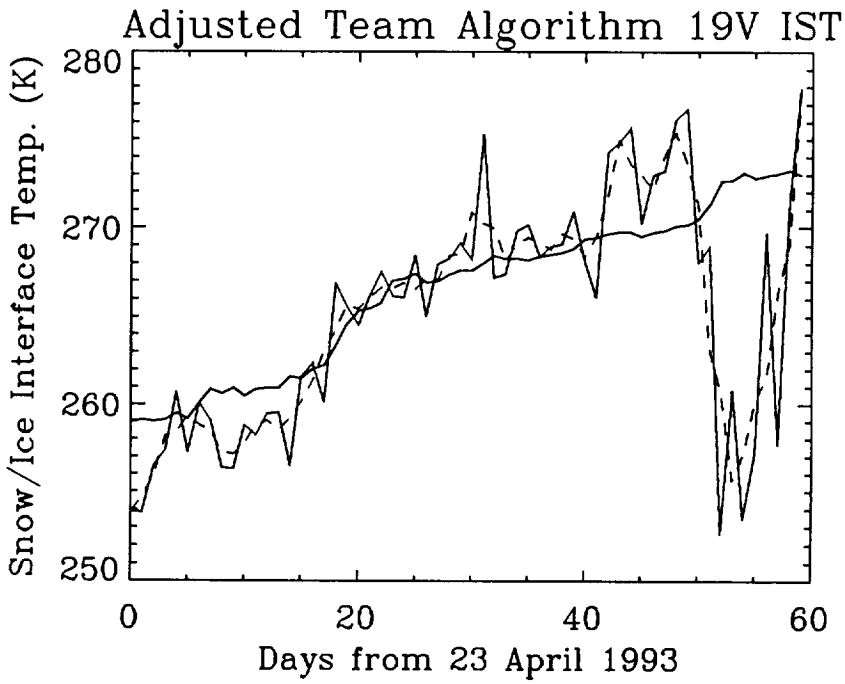

Fig. 5. Same as Figure 4, but with the Team Algorithm output adjusted to indicate 100% total ice cover (but with differing proportions of ice type). The thin solid line is the SSM/I temperatures. The dashed line is a 3-day running mean of the SSM/I temperatures.

In summary, our preliminary conclusions are that SSM/I data can provide useful ISTs if the surface types and emissivities are known, but that uncertainties in ice classification within the pack ice need to be reduced by some means, perhaps through combination with SAR data. An important point is that since atmospheric effects appear small enough to be neglected, differences between SSM/I temperatures and AVHRR-derived temperatures provides some information about the actual conditions of the surface. For example, if the SSM/I-derived ISTs are too large and too variable, then this implies a misclassification of ice concentration and/or ice type by the Team Algorithm. This knowledge might be used to constrain the Team Algorithm, perhaps by inverting the ice temperature algorithm to determine the proportions of ice type mixtures that match the estimated AVHRR temperatures. The SSM/I data might also prove useful for identifying significant changes in the ice-pack temperature profile during melt onset.

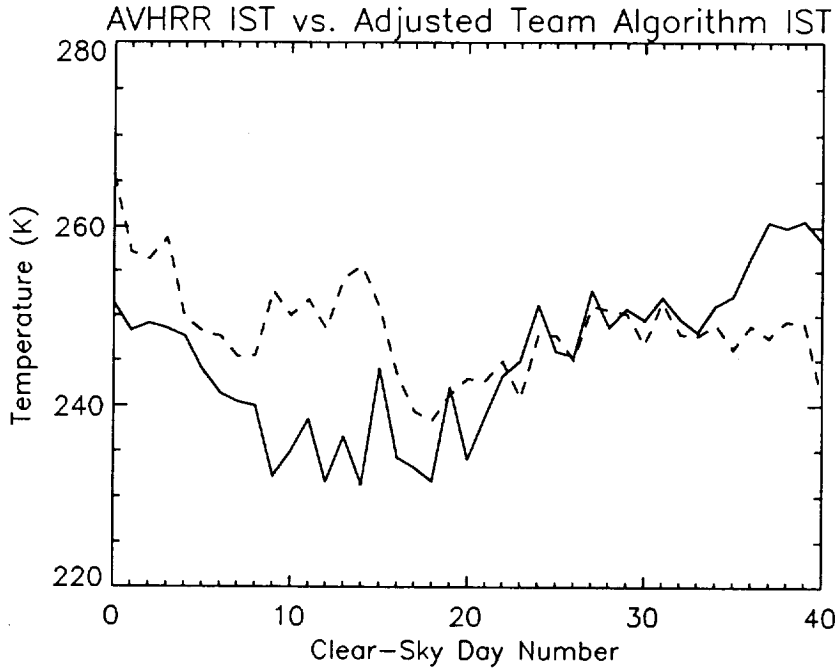

Fig. 6. Time series of AVHRR-derived temperatures and SSM/I-derived temperatures for clear-sky pixels in the Beaufort Sea data set. The solid line depicts the AVHRR temperatures. The SSM/I temperatures shown were derived using ice concentrations from the NASA Team Algorithm, but with the open-water fraction adjusted to be a fixed mixture of open water and young ice. A fixed adjustment was also applied to the surface-type emissivities, with each emissivity increased by about 10% from values cited in the literature.

3.0 PROGRESS TO DATE: PRODUCT GENERATION

3.1 Production of Ice Temperature Fields for the Polar Regions

Orbital AVHRR Global Area Coverage (GAC) imagery for two two-week periods were navigated, calibrated, and composited into 4.4 km grids covering both polar regions from 55 degrees North to the North Pole, and from 55 degrees South to the South Pole. The composited products (a total of 25 Gbytes) include the five AVHRR channels, time of acquisition, solar angles, and sensor viewing angles for each pixel. The CASPR cloud masking and ice temperature retrievals have been applied to a subset of these composites.

Procedures and software to extract, navigate, calibrate, and composite the GAC data were refined, including new tools and IDL routines to automate the steps. Several means of improving the efficiency of the processing were identified. The desired gridded products have been generated for a test period, and the resulting gridded products (individual swaths and composites) are available for distribution to other users. Ice temperatures and cloud masks have been derived successfully, although further adjustments in the cloud

masking scheme are needed to address the large range of conditions encountered within the composites. Compositing to GMT time as opposed to local time also introduces some spatial inconsistencies in the output, as the differences in local time produce a sharp boundary between clear and cloudy-sky areas.

Figure 7 gives an example of the GAC composites for a 12Z on 31 August 1984. Note that while the target time is 12Z, the composites may actually have data from 6Z to 18Z, depending on the scan angle/time combined decision rule (detailed in the Year 1 Annual Report). When IST retrievals are done with these composites, any time period within this range can be used. For example, we may choose to use only those pixels acquired within one hour of the target time. Of course, the shorter this period is, the fewer the cloud-free pixels, and the longer the compositing time (days) that will be required for reliable statistics.

3.2 Year-long Beaufort Sea ISTs

The 1992-93 Beaufort Sea data set, while not in our original plans, has turned out to be a particularly valuable resource. It covers all seasons on a daily basis (albeit with a two month gap) at LAC resolution, is well-calibrated, has co-located SSM/I data, and will eventually have the TOVS data stripped from the data stream and processed into temperature and humidity profiles. In short, there is no other data set like it. It is the test data set for CASPR, from which the surface temperatures shown in Figure 2 were computed. Various parameters are being retrieved from this data set for the RADARSAT GPS testing, and we will make our temperature products available to the scientific community.

3.3 Blended AVHRR-*In Situ* IST Product

While one of our original objectives was to generate a clear-sky ice surface temperature product from AVHRR data, this goal has been modified somewhat as a result of discussions that took place at the Workshop on Polar Data Sets, Seattle (October 1993). A blended product based on AVHRR clear-sky and drifting buoy temperatures generated considerable interest. Whether or not other data sources can be incorportated - e.g., TOVS or SSM/I - is yet to be determined.

The detailed structure of the blended product is uncertain at present, although it will be similar to the sample AVHRR product discussed previously. Its temporal coverage will depend upon the availability of data (probably from the Pathfinder activity) as well as funding for data processing since this was not part of our original budget.

Seelye Martin of the University of Washington has prepared a surface temperature product for the Arctic based on station and drifting buoy temperatures. Some of that data is shown in Figure 2. We will work with him on blending our two products.

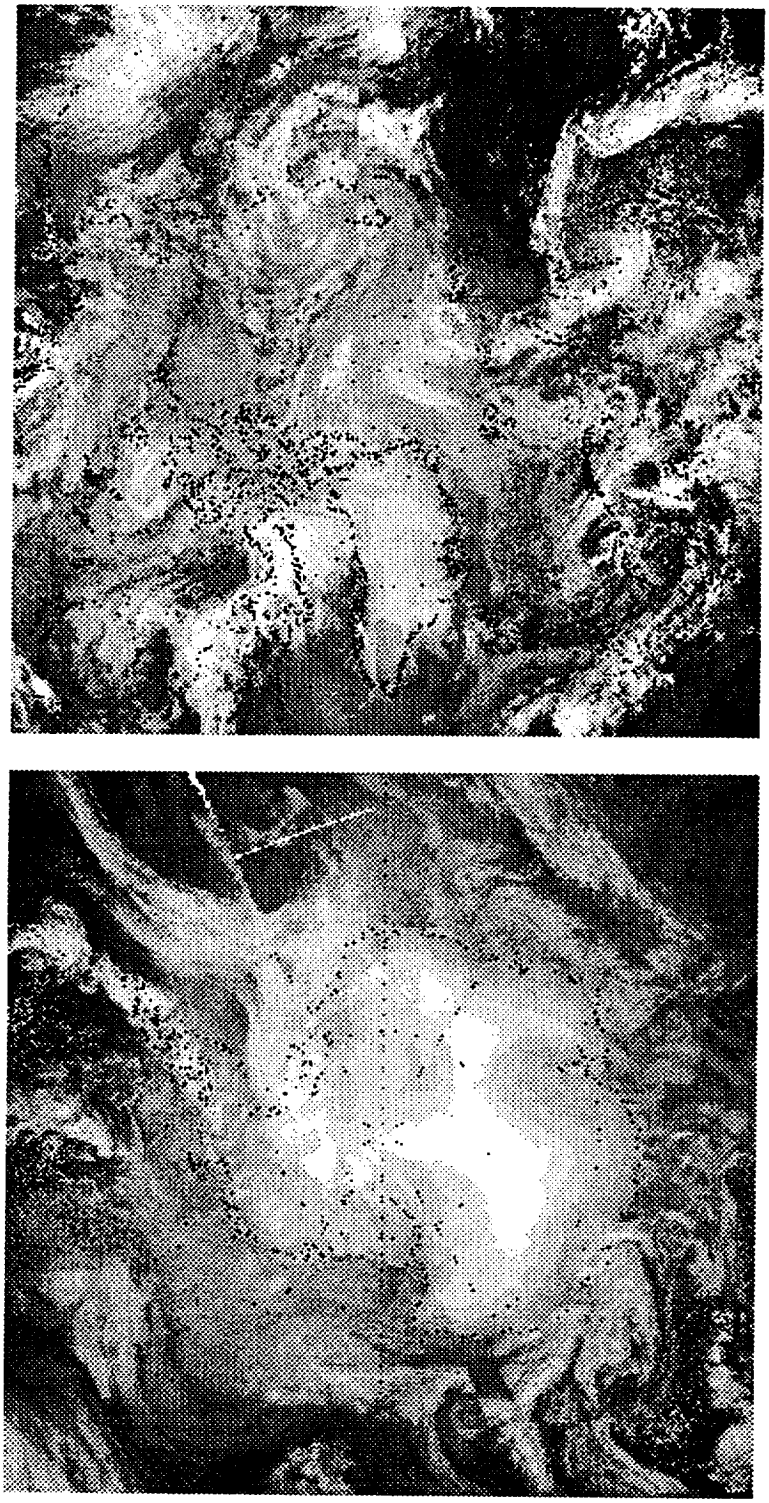

Fig. 7. AVHRR channel 4 brightness temperature composites with a target time of 12Z on 31 August 1984 for the Arctic (top) and Antarctic (bottom).

4.0 PLANS

During the third and final project year we will continue along these same lines although there will be an increased emphasis on product generation. Work is underway to validate and refine the geophysical algorithms as applied to the GAC composites. Other comparison data sets are being assembled (buoy observations, reanalyzed temperature fields, and gridded meteorological surface air temperatures).

The SSM/I results are positive enough to warrant some additional work. The SIMMS comparison will be expanded to include the 1992 field data, and we plan to pursue some methods to minimize the uncertainties in ice classification and emissivity assignment, including comparing aircraft microwave data with skin temperatures. Even with such improvements, it is unlikely that SSM/I IST can be retrieved with an accuracy better than perhaps 2 K. Accuracies would be greater with a higher-resolution instrument capable of reducing the variability in proportions of surface types within the field of view. The problem remains that a given percent error in emissivity yields an equivalent error in estimated IST, and a precise knowledge of emissivity is probably impossible to obtain without surface measurements. Since emissivity varies relatively little with ice type at low microwave frequencies, use of a 6 or 10 Ghz channel (such as planned for MIMR) would improve the IST estimates.

5.0 PUBLICATIONS SUPPORTED IN WHOLE OR PART BY THIS GRANT

Key, J., J.A. Maslanik, T. Papakyriakou, M.C. Serreze, and A.J. Schweiger. On the validation of satellite-derived sea ice surface temperature. *Arctic*, 47(3), 280-287.

Key, J., High-latitude surface temperature estimates from thermal satellite data, In preparation for *J. Geophys. Res. (Oceans)*.

6.0 REFERENCES

Munoz, E.A. and S. Martin, 1995, Gridded Arctic surface temperature data sets: a comparison with Soviet ice station and land temperatures for 1987-88, *J. Climate* (submitted).